

Classification of Brain Tumors by Nanopore Sequencing of Cell-Free DNA from Cerebrospinal Fluid

Ann-Kristin Afflerbach,^{a,b} Christian Rohrandt,^c Björn Brändl,^d Marthe Sönksen,^a Jürgen Hench,^e Stephan Frank,^e Daniela Börnigen,^f Malik Alawi,^f Martin Mynarek ,^a Beate Winkler,^a Franz Ricklefs ,^g Michael Synowitz,^h Lasse Dührsen,^g Stefan Rutkowski,^a Annika K. Wefers ,^{i,j} Franz-Josef Müller,^{d,k} Melanie Schoof ,^{a,b,t} and Ulrich Schüller ,^{a,b,i,*t}

BACKGROUND: Molecular brain tumor diagnosis is usually dependent on tissue biopsies or resections. This can pose several risks associated with anesthesia or neurosurgery, especially for lesions in the brain stem or other difficult-to-reach anatomical sites. Apart from initial diagnosis, tumor progression, recurrence, or the acquisition of novel genetic alterations can only be proven by re-biopsies.

METHODS: We employed Nanopore sequencing on cell-free DNA (cfDNA) from cerebrospinal fluid (CSF) and analyzed copy number variations (CNV) and global DNA methylation using a random forest classifier. We sequenced 129 samples with sufficient DNA. These samples came from 99 patients and encompassed 22 entities. Results were compared to clinical diagnosis and molecular analysis of tumor tissue, if available.

RESULTS: 110/129 samples were technically successful, and 50 of these contained detectable circulating tumor DNA (ctDNA) by CNV or methylation profiling. ctDNA was detected in samples from patients with progressive disease but also from patients without known residual disease. CNV plots showed diagnostic and prognostic alterations, such as *C19MC* amplifications in embryonal tumors with multilayered rosettes or Chr.1q gains and Chr.6q losses in posterior fossa group A ependymoma, respectively. Most CNV profiles mirrored the profiles of the respective tumor tissue. DNA methylation allowed exact classification of the tumor in 22/110 cases and led to incorrect classification in

2/110 cases. Only 5/50 samples with detected ctDNA contained tumor cells detectable through microscopy.

CONCLUSIONS: Our results suggest that Nanopore sequencing data of cfDNA from CSF samples may be a promising approach for initial brain tumor diagnostics and an important tool for disease monitoring.

Introduction

Central nervous system (CNS) tumors are very heterogeneous and can be classified into more than 100 different entities, according to the most recent 2021 World Health Organization guidelines (1). For treatment planning, it is essential to diagnose the exact type and subtype of the tumor. Here, the diagnosis heavily relies on the histological characteristics of the tumor. More recently, sequencing technologies and DNA methylation analyses have become valuable if not essential tools for diagnostics. Sequencing may identify diagnostic hallmarks or targetable alterations in a tumor. However, robust estimations on the molecular tumor entity are hard to obtain from sequencing alone, as tumor entities may not be characterized by specific single nucleotide variants or gene fusions. By global DNA methylation profiling, thousands of CpG sites within the genome are evaluated, resulting in a multidimensional fingerprint of the tumor. This signature can then be compared with reference databases to determine the highest similarity of the sample to a specific CNS tumor entity (2). As opposed to

^aDepartment of Pediatric Hematology and Oncology, University Medical Center Hamburg-Eppendorf, Hamburg, Germany;

^bResearch Institute Children's Cancer Center Hamburg, Hamburg, Germany; ^cInstitute for Communications Technologies and Embedded Systems, University of Applied Sciences Kiel, Kiel, Germany; ^dCenter for Integrative Psychiatry, University Hospital Schleswig-Holstein, Kiel, Germany; ^eDepartment of Pathology, University Hospital Basel, Basel, Switzerland; ^fBioinformatics Core, University Medical Center Hamburg-Eppendorf, Hamburg, Germany; ^gDepartment of Neurosurgery, University Medical Center Hamburg-Eppendorf, Hamburg, Germany; ^hDepartment of Neurosurgery, University Hospital Schleswig-Holstein, Campus Kiel,

Kiel, Germany; ⁱInstitute of Neuropathology, University Medical Center Hamburg-Eppendorf, Hamburg, Germany; ^jMildred Scheel Cancer Career Center HaTriCS4, University Medical Center Hamburg- Eppendorf, Hamburg, Germany; ^kDepartment of Genome Regulation, Max Planck Institute for Molecular Genetics Berlin, Berlin, Germany.

*Address correspondence to this author at: Research Institute Children's Cancer Center Hamburg, Martinistraße 52, N63 (LIV), D-20251 Hamburg, Germany. E-mail: u.schueler@uke.de.

^tThese authors contributed equally to this work.

Received March 7, 2023; accepted June 28, 2023.

<https://doi.org/10.1093/clinchem/hvad115>

sequencing analyses, this technique indeed holds the potential of an exact molecular tumor classification.

A drawback for current CNS tumor diagnostics is the potential unavailability of tissue biopsies due to the tumor location or risks associated with surgery. In such cases, oncologists are left with imaging results and molecularly unclear diagnoses, such as diffuse intrinsic pontine glioma. Also, relapses or metastases of a previously diagnosed primary CNS tumor may be evident from magnetic resonance imaging, but early detection and distinction from radiation-induced changes or secondary tumors can be challenging. Furthermore, molecular changes of a tumor requiring adjuvant treatment adaptations are impossible to identify without re-biopsy. Collectively, this highlights the need for novel diagnostic methods that allow exact molecular tumor characterization without invasive tissue biopsies.

In this regard, liquid biopsies have become popular for various cancer entities. Recently, the research on analytes from liquid biopsies, such as circulating tumor cells and cell-free DNA (cfDNA) were included in a multitude of clinical trials (3). Although detection of circulating tumor cells and cfDNA of brain tumors in peripheral blood is possible (4, 5), cerebrospinal fluid (CSF) is preferred for the diagnosis and monitoring of CNS tumors. Disease monitoring of medulloblastoma by CSF microscopy is standard-of-care in many countries, although many patients develop solid metastases along the cerebrospinal axis in the absence of tumor cells in CSF microscopy. cfDNA, a relatively stable and thereby promising analyte from CSF, can recapitulate copy number changes of the tumor by whole genome low-coverage sequencing (6–8) and can serve as a prognostic marker for minimal residual disease (8). However, such methods are still time consuming and costly, and they may not provide sufficiently reliable information on a tumor entity for initial diagnosis.

Nanopore sequencing is a third-generation sequencing technology that has initially been developed for long reads. However, since the method has now been adapted for shorter reads, it provides the possibility of copy number variation (CNV) and methylation analysis of cfDNA (9, 10). The low starting cost and easy handling make Nanopore sequencing an attractive complement to current standard diagnostic methods. In this study, we employed low-coverage Nanopore sequencing for CNV and methylation analysis in a cohort of 129 CSF-derived cfDNA samples. We show that this strategy has the power of noninvasive, molecular brain tumor diagnostics including initial testing prior to surgery and disease monitoring during and after treatment.

Material and Methods

SAMPLE COLLECTION

CSF was collected from patients with brain tumors or suspected brain tumors for routine diagnostics.

Standard tubes were used, and time from collection to processing was unknown in most cases. Samples were processed in the neuropathology department for cytology analysis by centrifuging for 10 min at 750 $\times g$. The sediment was used for routine diagnostics, and 0.5 to 5 mL supernatant was frozen at -20°C until further processing. The use of biopsy specimens for research upon anonymization was in accordance with local ethical standards and regulations at the University Medical Center Hamburg-Eppendorf.

CFDNA ISOLATION

For cfDNA isolation, CSF supernatant was thawed at room temperature and centrifuged for 10 min at 11 000 $\times g$. cfDNA isolation was performed using the Qiagen QIAamp Circulating Nucleic Acid kit or the Macherey-Nagel NucleoSnap cfDNA kit. Total DNA content of the isolated DNA was measured using the Invitrogen Qubit 3.0 with the High Sensitivity DNA assay. cfDNA fragment size distribution was determined on samples with sufficient DNA using the Agilent High Sensitivity DNA kit for the BioAnalyzer. The region for cfDNA calculation was set to 75 to 400 bp. Isolated cfDNA was stored at -20°C until sequencing.

NANOPORE SEQUENCING OF CFDNA

cfDNA was prepared for sequencing using the Oxford Nanopore SQK-LSK110 sequencing kit (for details see [Supplemental Methods](#)). Samples were processed individually on FLO-MIN106 R.9.4.1 flow cells on a MinION Mk1B or Mk1C device. Minimum read length was set to 20 bp. Read length and quality were evaluated with NanoPlot 1.33.0 (11).

DNA METHYLATION PROFILING OF TUMOR TISSUE

DNA from tissue was evaluated for the methylation status of 850 000 CpG sites using the MethylationEPIC BeadChip on an iScan device, both by Illumina. Details are described in [Supplemental Methods](#).

CNV ANALYSIS

Fastq files were generated using the Guppy 6.1.5 model for samples sequenced on MinION Mk1b, and Guppy 6.3.8 for samples sequenced on MinION Mk1C. Files were aligned to the human genome hg38 using Minimap 2.17 (12, 13) with -ax map-ont settings. Sam files were transformed and sorted using samtools 1.15.1 (14). Bam files were analyzed for CNVs using Control-FREEC 11.6 (15). Window size was set to 150k bp if the number of passed reads surpassed 500k; otherwise, window size was set to 500k bp. Results were plotted in R using the packages magrittr, tidyverse, karyoploteR, and scales. Each dot represents a window of 150k bp or 500k bp; color was defined by the median

ratio of each segment. Empirical threshold for a gain was >1.1 and for a loss was <0.9 .

NANODX ANALYSIS AND UNIFORM MANIFOLD

APPROXIMATION AND PROJECTION VISUALIZATION

Fast5 files were basecalled using the Guppy 4.4.2 model, and methylation status was called using nanoprocess 0.13.2 (16). Sequences were aligned to the reference genome hg38 p13 with Minimap 2.22 (12, 13). The NanoDx pipeline (17) was employed for methylation analysis and tumor classification, with a minimum data requirement of 1000 detected CpG sites. Binarized methylation was visualized in uniform manifold approximation and projection. Details are described in [Supplemental Methods](#).

CALCULATION OF TUMOR FRACTION

Tumor fraction of samples was calculated using ichorCNA (18) on aligned bam files of the Nanopore data. Tumor fraction with the highest log likelihood is reported.

Results

ISOLATION AND ANALYSIS OF CELL-FREE DNA FROM ROUTINE CEREBROSPINAL FLUID SAMPLES

We collected and attempted analysis on 178 CSF samples from patients with CNS tumors ([Fig. 1A](#)). One hundred fifty-one of 178 samples (86%) had a volume of >1 mL, making those suitable for cfDNA isolation. Of these, 129/178 samples (85%) contained at least 5 ng DNA, making them suitable for Nanopore sequencing. Nineteen of 129 samples (15%) did not achieve >100000 passed reads and were therefore considered a technical failure ([Fig. 1A](#)).

We sequenced 129 CSF samples from 99 patients ([Fig. 1B](#), [Supplemental Table 1](#)). Our cohort comprises 22 different entities, with medulloblastoma being the largest group ($n = 49/129$, 38%), followed by ependymoma ($n = 17/129$, 13.2%) and pilocytic astrocytoma ($n = 11/129$, 8.5%). Rarer tumors included atypical teratoid rhabdoid tumors ($n = 8/129$, 6.2%) or embryonal tumors with multilayered rosettes (embryonal tumor with multilayered rosettes, $n = 3/129$, 2.3%). The median age was 19.2 years, with the majority of patients being children or adolescents ($n = 91/129$, 70.5%), reflecting that CSF analysis is standard-of-care for most pediatric patients but is less common for adult patients with primary brain tumors.

Forty-one of 129 samples (31.8%) were collected prior to surgery; 26/129 (20.2%) samples were from early post-surgery (<14 days), and 61/129 (47.3%) samples were from later after surgery (≥ 14 days). For sample #65, information on the sampling time was not

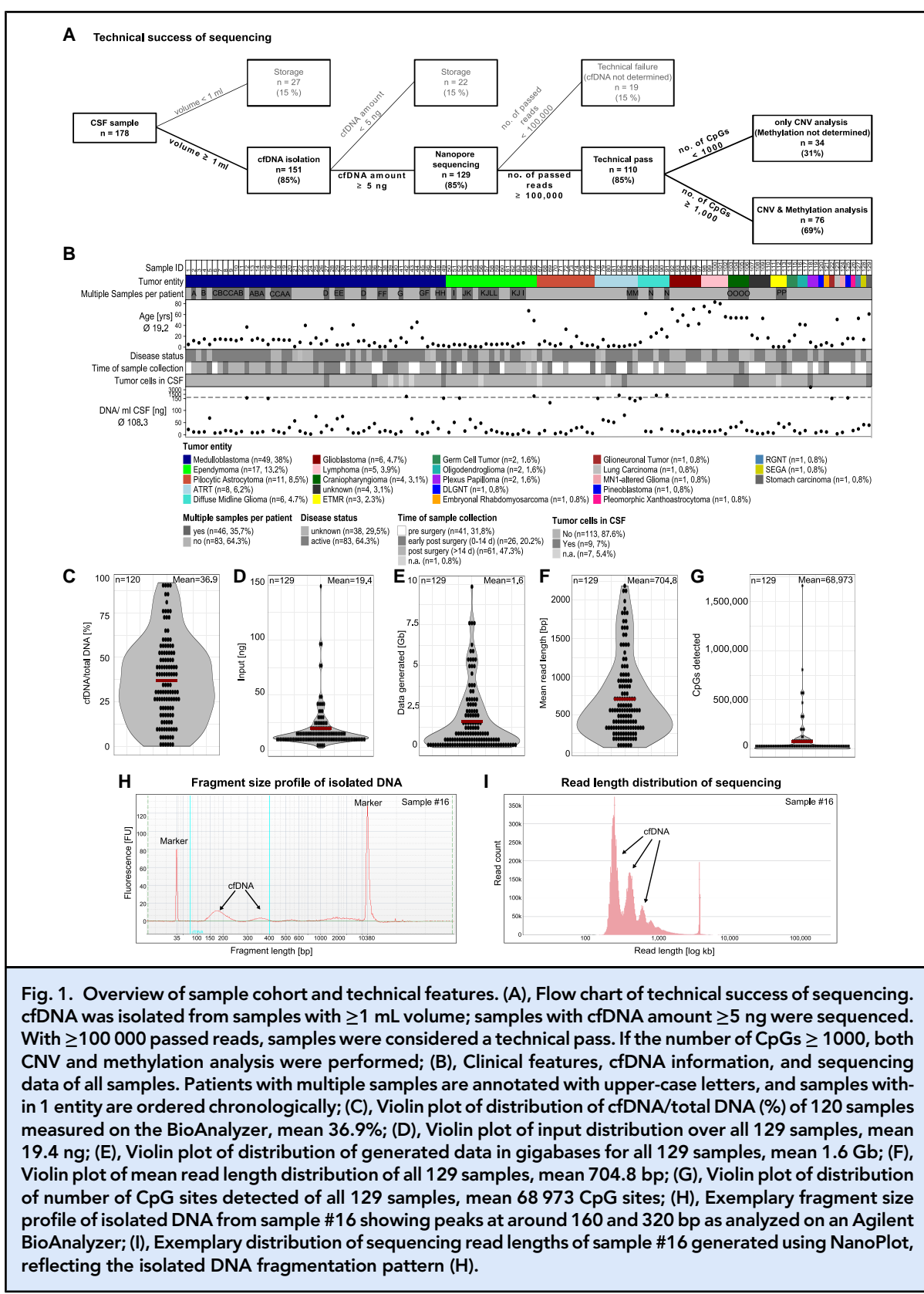
available. Only 9/122 samples with information on histological examination of tumor cells in the CSF (7.4%) contained microscopically detectable tumor cells ([Fig. 1B](#)).

Between 1.5 and 3,835 ng DNA per ml CSF were isolated (mean: 108.3 ng DNA; median: 16.2 ng DNA). cfDNA percentage of total isolated DNA, defined as the proportion of DNA within 75 to 400 bp detected with the BioAnalyzer, ranged from 0% to 92%, with a mean cfDNA proportion of 36.9% ([Fig. 1C](#), exemplary distribution of sample #16 in [Fig. 1H](#)). The input ranged from 3 to 97.8 ng, with a mean of 19.4 ng ([Fig. 1D](#)). On average, 1.77 gigabases were sequenced per sample ([Fig. 1E](#)), which reflects a coverage of 0.5x, with an overall mean read length of 704.8 bp ([Fig. 1F](#)). The number of detected CpG sites ranged between 0 and 1 663 380 CpG sites for all samples (mean: 68 973, [Fig. 1G](#)). The mean read length was also reflective of the percentage of cfDNA in the sequenced sample ([Fig. 1I](#)).

CIRCULATING TUMOR DNA DETECTABLE BY NANOPORE SEQUENCING IN PRE- AND EARLY POST-SURGERY CSF SAMPLES

First, cfDNA of the 67/129 CSF samples collected pre- and early post-surgery were sequenced to determine the success rate of the method, as in either scenario tumor cells should potentially shed circulating tumor (ctDNA) into the CSF. CNV plots were generated, and methylation analysis performed using the NanoDx classifier (17) ([Fig. 2A](#)). ctDNA was detected in 30/67 samples (45%). In 15/67 samples (22%) ctDNA was detected by CNV alone, in 12/67 samples (18%) by both CNV and methylation profiling, and in 3/67 samples (5%) only by methylation profiling ([Fig. 2B](#)).

Whenever ctDNA was detected in the CSF, it accurately replicated the CNV profile of the tumor determined by methylation array analysis in most cases, as illustrated in [Fig. 2C](#) for a glioblastoma (sample #95) and for all samples with ctDNA detection by CNV profiling in [Supplemental Fig. 1](#). With a NanoDx score of 0.072 and clear clustering with glioblastoma in uniform manifold approximation and projection visualization, sample #95 was correctly classified by both analysis methods. We also detected some cases with alterations that were private to either the tumor tissue or the CSF ([Fig. 2D](#), [Supplemental Fig. 1](#)). For example, for a group 4 medulloblastoma (sample #16), we found a chr. 2 gain private to the cfDNA profile and a chr. 3 loss detected only in the tissue ([Fig. 2D](#), asterisks). Moreover, in sample #113, we were able to correctly predict the tumor class by methylation analysis with a NanoDx score of 0.148, but we also detected a *C19MC* amplification in the CNV, which is diagnostically relevant for embryonal tumor with multilayered rosettes ([Fig. 2E](#)).



Brain Tumor Classification from CSF

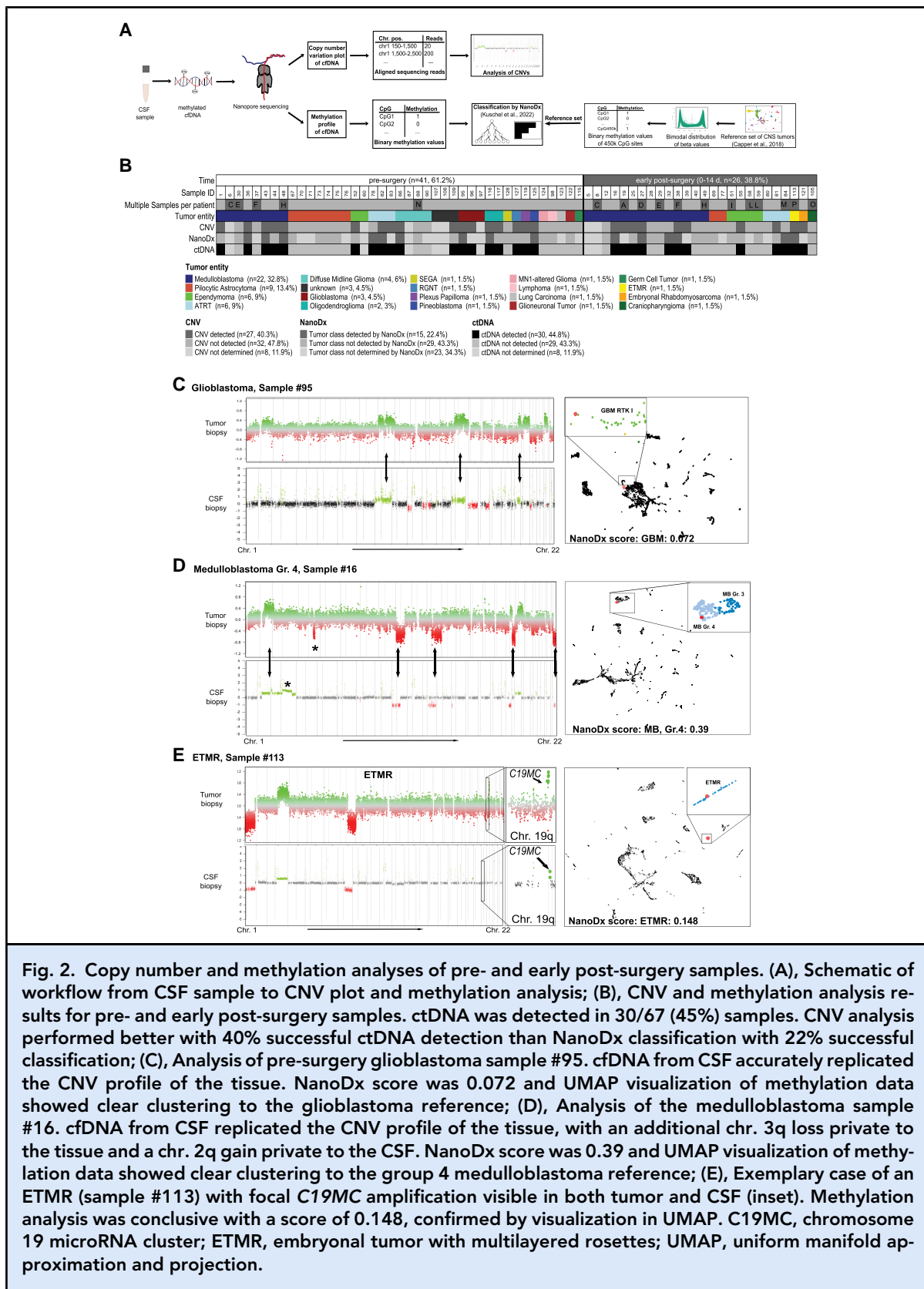


Fig. 2. Copy number and methylation analyses of pre- and early post-surgery samples. (A), Schematic of workflow from CSF sample to CNV plot and methylation analysis; (B), CNV and methylation analysis results for pre- and early post-surgery samples. ctDNA was detected in 30/67 (45%) samples. CNV analysis performed better with 40% successful ctDNA detection than NanoDx classification with 22% successful classification; (C), Analysis of pre-surgery glioblastoma sample #95. cfDNA from CSF accurately replicated the CNV profile of the tissue. NanoDx score was 0.072 and UMAP visualization of methylation data showed clear clustering to the glioblastoma reference; (D), Analysis of the medulloblastoma sample #16. cfDNA from CSF replicated the CNV profile of the tissue, with an additional chr. 3q loss private to the tissue and a chr. 2q gain private to the CSF. NanoDx score was 0.39 and UMAP visualization of methylation data showed clear clustering to the group 4 medulloblastoma reference; (E), Exemplary case of an ETMR (sample #113) with focal C19MC amplification visible in both tumor and CSF (inset). Methylation analysis was conclusive with a score of 0.148, confirmed by visualization in UMAP. C19MC, chromosome 19 microRNA cluster; ETMR, embryonal tumor with multilayered rosettes; UMAP, uniform manifold approximation and projection.

In only 2 cases, sample #75, a pilocytic astrocytoma, and sample #127, a rosette-forming glioneuronal tumor, methylation analysis classified the tumor incorrectly with scores of 0.073 and 0.0921 to lymphoma and meningioma, respectively.

ctDNA DETECTION IN POST-SURGERY SAMPLES SERVES AS AN INDICATOR FOR DISEASE PROGRESSION OR RELAPSE

Next, we investigated the 61/129 samples that were collected post-surgery. This included several patients with multiple samples (Fig. 3A, annotated with capital letters). Time after surgery ranged from 14 to 9818 days, with a median of 205 days. Nanopore sequencing was technically successful in 50/61 cases (82%), and ctDNA was detected by at least one method in 20/61 cases (32.8%, Fig. 3A). CNV analysis revealed the presence of ctDNA in 17/61 samples (27.9%), whereas methylation analysis only classified the correct tumor in 7/61 samples (11.5%).

Longitudinal studies have shown that CSF-derived cfDNA is a powerful tool for tumor monitoring (8). We replicated this for 2 patients within our cohort using Nanopore sequencing (Fig. 3, B and C). Patient A (Fig. 3B) had a wingless-activated medulloblastoma harboring a *CTNNB1* p.S37A mutation. Subtyping of this tumor was difficult, as the highest score varied depending on the brain tumor classifier version (wingless-activated in v11b4 but group 3 in v12.5, www.molecularneuropathology.org). After a short period of complete remission, a solid metastasis at the wall of the lateral ventricle was discovered. CSF taken during the following phase of progressive disease showed ctDNA that, in addition to the copy number alterations of the initial tumor tissue, exposed loss of chr. 10 (asterisk, sample #2). Methylation profiling classified the tumor as group 3 medulloblastoma by NanoDx, which is also reflected in uniform manifold approximation and projection clustering. During a stable disease phase in therapy, CNV analysis of the cfDNA showed a flat genome and the methylome clustering to control tissue (sample #10). With recurrent disease progression starting again at day 883, a second surgery was needed. The loss of chr. 10, previously only detected in the CSF, was now detected in the tumor tissue. In addition, the tumor now harbored a chr. 2p gain (asterisk), and, again, the tissue DNA methylation profile had features of both wingless-activated and group 3 medulloblastoma. After this second surgery, ctDNA was detected in CSF sample #20 at day 990, showing precisely the CNV profile of the relapse tissue, including the chr. 2p gain.

The power of liquid biopsies for tumor monitoring was also evident in the case of patient G (Fig. 3C), a 5-year-old child with a posterior fossa group A ependymoma. Initial tumor biopsy showed a chr. 1q gain, known to indicate worse overall survival (19), and a chr. 8 gain (asterisk). Three weeks after surgery,

CSF-derived cfDNA revealed an additional chr. 6q loss (asterisk), while the chr. 8 gain disappeared (sample #53). The methylation analysis of this sample was inconclusive but still showed the highest NanoDx score for posterior fossa group A ependymoma (0.05). The combination of chr. 1q gain and chr. 6q loss, which had been associated with an ultra-high risk (19), was then confirmed in a second surgery 6 months after its detection in the cfDNA. Three months after second surgery, no ctDNA was detected by CNV or NanoDx (sample #57), suggesting remission.

ctDNA DETECTION IN 50/129 (39%) OF ALL ANALYZED CSF SUPERNATANTS

Overall, ctDNA was detected in 50/129 samples (39%) and in 50/110 technically successful samples (45%) by at least one analysis method (Fig. 4, A and B). As an indicator of success, a high fraction of cfDNA per total DNA was correlated with the detection of ctDNA (*t*-test, $P=0.011$, Fig. 4C), as was a higher tumor fraction calculated by ichorCNA (*t*-test, $P=9.6\times10^{-7}$, Fig. 4D) as well as a shorter read length (*t*-test, $P=0.0042$, Fig. 4E). Comparing the detection rates of both methods and CNV and NanoDx alone in respect to the fraction of cfDNA as well as calculated tumor fraction revealed that a high proportion of tumor DNA is significantly correlated with detection by both methods. Neither of the 2 methods alone is significantly more sensitive (Supplemental Fig. 2).

In general, ctDNA of benign tumors including CNS World Health Organization grade 1 and 2 entities was detected in 15% of the cases, whereas malignant tumors were detectable in 48% of our samples ($P=0.003$, Fig. 4F).

To evaluate the performance of CNV and methylation analysis by NanoDx, we compared the method of detection (Fig. 4G). Thirty-two percent of cases ($n=16/50$) were detected and correctly classified by both methods. CNV analysis detected ctDNA in an additional 28/50 cases (56%), and NanoDx did so in an additional 6/50 cases (12%). Of note, 4 samples in our cohort (#103–#106) were taken from a patient with a tumor not harboring any CNVs. Hence, detecting ctDNA through CNV analysis was not possible.

The percentage of cfDNA per total DNA did not differ significantly between the 7 largest groups of tumor entities, which included aggressive entities, such as medulloblastoma and atypical teratoid rhabdoid tumors, as well as less aggressive entities like pilocytic astrocytoma (Kruskal-Wallis test, $P=0.54$, Fig. 4H). Neither did the percentage of passed reads differ among these groups, although atypical teratoid rhabdoid tumor samples showed a trend toward more passed reads (Kruskal-Wallis test, $P=0.093$, Fig. 4I).

Brain Tumor Classification from CSF

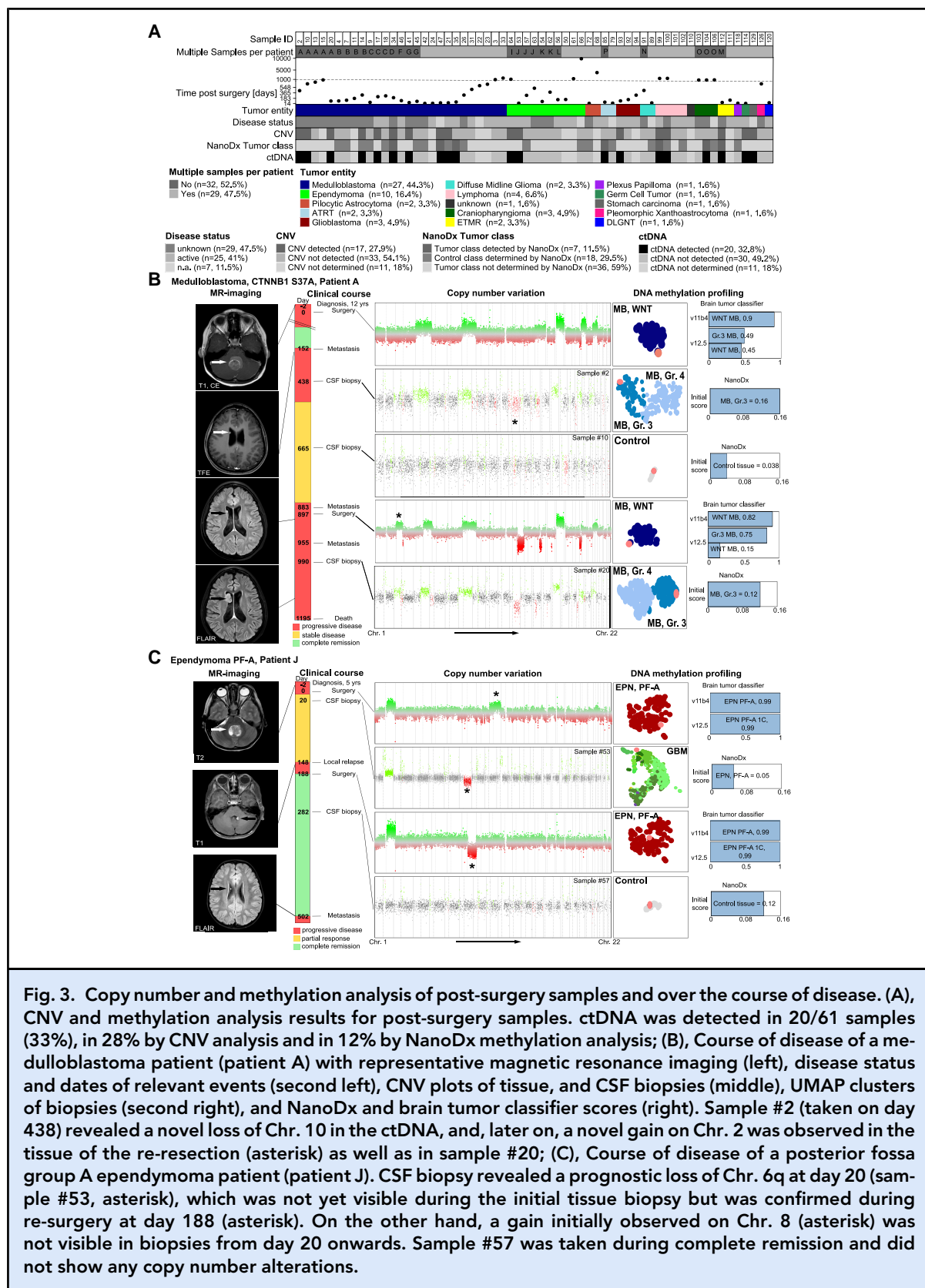


Fig. 3. Copy number and methylation analysis of post-surgery samples and over the course of disease. (A), CNV and methylation analysis results for post-surgery samples. ctDNA was detected in 20/61 samples (33%), in 28% by CNV analysis and in 12% by NanoDx methylation analysis; (B), Course of disease of a medulloblastoma patient (patient A) with representative magnetic resonance imaging (left), disease status and dates of relevant events (second left), CNV plots of tissue, and CSF biopsies (middle), UMAP clusters of biopsies (second right), and NanoDx and brain tumor classifier scores (right). Sample #2 (taken on day 438) revealed a novel loss of Chr. 10 in the ctDNA, and, later on, a novel gain on Chr. 2 was observed in the tissue of the re-resection (asterisk) as well as in sample #20; (C), Course of disease of a posterior fossa group A ependymoma patient (patient J). CSF biopsy revealed a prognostic loss of Chr. 6q at day 20 (sample #53, asterisk), which was not yet visible during the initial tissue biopsy but was confirmed during re-surgery at day 188 (asterisk). On the other hand, a gain initially observed on Chr. 8 (asterisk) was not visible in biopsies from day 20 onwards. Sample #57 was taken during complete remission and did not show any copy number alterations.

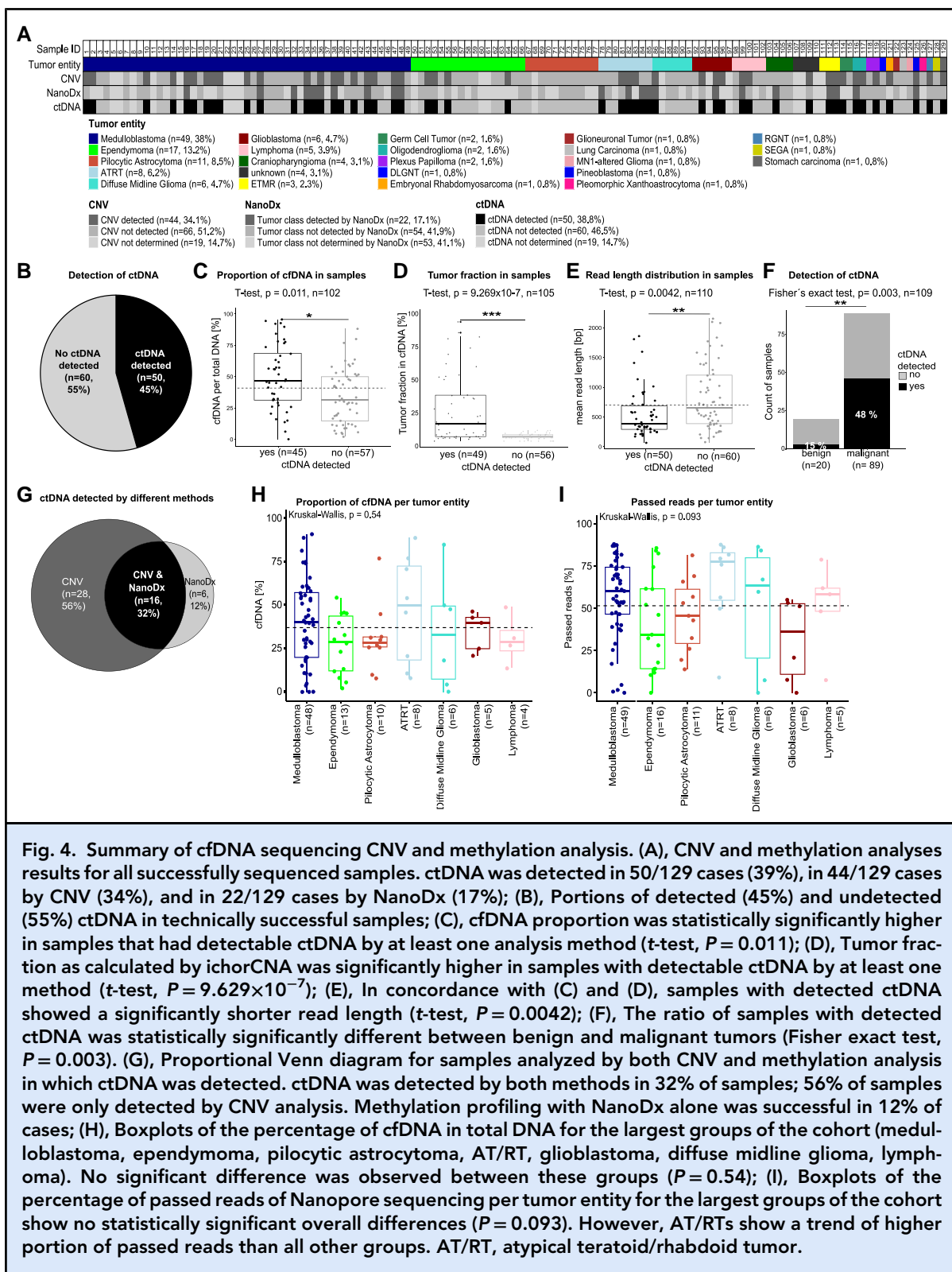


Fig. 4. Summary of cfDNA sequencing CNV and methylation analysis. (A), CNV and methylation analyses results for all successfully sequenced samples. ctDNA was detected in 50/129 cases (39%), in 44/129 cases by CNV (34%), and in 22/129 cases by NanoDx (17%); (B), Portions of detected (45%) and undetected (55%) ctDNA in technically successful samples; (C), cfDNA proportion was statistically significantly higher in samples that had detectable ctDNA by at least one analysis method (t-test, $P = 0.011$); (D), Tumor fraction as calculated by ichorCNA was significantly higher in samples with detectable ctDNA by at least one method (t-test, $P = 9.629 \times 10^{-7}$); (E), In concordance with (C) and (D), samples with detected ctDNA showed a significantly shorter read length (t-test, $P = 0.0042$); (F), The ratio of samples with detected ctDNA was statistically significantly different between benign and malignant tumors (Fisher exact test, $P = 0.003$). (G), Proportional Venn diagram for samples analyzed by both CNV and methylation analysis in which ctDNA was detected. ctDNA was detected by both methods in 32% of samples; 56% of samples were only detected by CNV analysis. Methylation profiling with NanoDx alone was successful in 12% of cases; (H), Boxplots of the percentage of cfDNA in total DNA for the largest groups of the cohort (medulloblastoma, ependymoma, pilocytic astrocytoma, AT/RT, glioblastoma, diffuse midline glioma, lymphoma). No significant difference was observed between these groups ($P = 0.54$); (I), Boxplots of the percentage of passed reads of Nanopore sequencing per tumor entity for the largest groups of the cohort show no statistically significant overall differences ($P = 0.093$). However, AT/RTs show a trend of higher portion of passed reads than all other groups. AT/RT, atypical teratoid/rhabdoid tumor.

Discussion

An exact diagnosis of CNS tumors, which is crucial for clinical treatment and prognostic stratification, usually relies on tissue biopsies. Only biopsies allow a state-of-the-art integrated diagnosis including imaging as well as molecular and histological tumor data. However, the use of liquid biopsies holds great promise to improve patient care (20, 21). This is especially true for surgically inaccessible brain tumors eluding conventional molecular diagnostic approaches. For these tumors, inclusion of a molecular analysis of cfDNA would allow a diagnosis not solely relying on imaging. More recent data further indicate that molecular information on the tumor may impact surgery planning. This is not only true for lymphoma, where surgical resection is usually not recommended, but also relevant for glioblastoma, where the overall survival might not necessarily increase after gross total tumor resection depending on the molecular subclass of the tumor (22). Finally, a small residual tumor in medulloblastoma is not considered a relevant factor for risk of relapse (23), but the presence of any residual tumor is one of the key prognostic factors in ependymoma (24).

Additionally, liquid biopsies have already been described to be useful for minimal residual disease detection. The minimal residual disease detection by molecular methods is more sensitive than cytologic examinations, as shown by us and others (8). The clinical relevance of this has not yet been examined in detail but will likely be included into upcoming clinical trials.

We employed Nanopore sequencing for cfDNA from 129 routinely collected CSF samples spanning 22 different tumor entities, disease states, collection times, and malignancy grades. Samples were received without special tubes, at ambient temperature, and with unknown time between CSF tap and arrival in the lab, but we could still successfully sequence 110/129 of these samples (85%). A higher proportion of cfDNA in the sequenced DNA led to a significant improvement in ctDNA detection, suggesting that cfDNA in CSF is mostly derived from tumor cells.

ctDNA is fragmented into parts of 160 bp and multiples thereof. An in silico size selection of sequencing reads of plasma samples can increase the sensitivity of tumor detection (25). We could not recapitulate this in our CSF samples (*Supplemental Fig. 3*), most likely due to the low amount of DNA in CSF of healthy individuals (26). The presence of cfDNA in CSF may therefore per se hint toward inflammation or presence of a tumor.

By comparing pre-surgery and early post-surgery samples, we saw no differences in detection of ctDNA, e.g., due to surgical intervention, showing that both parts of the cohort are valid for methodological testing. Within the pre- and early post-surgery samples, we achieved a classification rate of 45% in technically successful samples. This highlights

the potential of the method for complementing initial diagnosis methods and potential implementation in clinical routines. Also, longitudinal studies for monitoring and detection of possible relapses are possible.

Using the results generated from sequencing and methylation profiling, we detected ctDNA in 50/129 samples (39%). In 44 of these 50 samples (88%), CNV analysis was informative. The additional generation of methylation profiles was helping significantly as it detected tumor DNA in an additional 6/50 (12%) of samples and as it was able to reliably classify tumors if tissue was not available. Neither CNV analysis nor methylation profiling show superior sensitivity, and both were able to detect samples with a low tumor DNA proportion. This further indicates the superiority of Nanopore sequencing over low-coverage sequencing. For the detection of specific mutations though, other methods, e.g., droplet digital polymerase chain reaction would need to complement Nanopore sequencing in a clinical setting, as Nanopore sequencing still has a relatively high failure rate, especially of short reads and inherent low coverage.

It has previously been shown that the CNV profiles generated from low-coverage sequencing of cfDNA from CSF may be informative of the tumor state and that copy number alterations may slightly change over the course of the disease (8). In our cohort, most CNV profiles generated from cfDNA resembled the CNV profile from the matching tumor biopsy. Only in some cases, we detected changes specific to either the tumor or the ctDNA in the CSF. Still, the clinical meaning of such changes needs to be further addressed as well as the question of whether such changes reflect altered subclone fractions and whether they have developed de novo or totally disappeared. CNV analysis has inherent limitations as it will only indicate the presence of ctDNA if the tumor has chromosomal aberrations. Therefore, DNA methylation profiling is a suitable addition as it has become an extremely valuable tool for diagnosis of CNS tumors (2). Such analyses are usually generated by Illumina methylation arrays that require ≥ 100 ng DNA, which is not achievable for most CSF samples. Another method able to infer the methylation profile from small amounts of DNA is methylated DNA immunoprecipitation sequencing and specifically cell-free methylated DNA immunoprecipitation sequencing for cfDNA (27, 28). Still, Nanopore sequencing is significantly less time-, labor-, and cost-intensive compared to cell-free methylated DNA immunoprecipitation sequencing and can also be employed with small DNA amounts, making this our method of choice. For example, conventional sequencing approaches have a usual workflow of around 5 days (29), with similarly lengthy workflows for methylation analyses. Nanopore sequencing allows same-day or next-day results for tissue (30), as well as for CSF biopsies as described in our study.

The validity of Nanopore sequencing for the analysis of global DNA methylation has only recently been demonstrated (17). Kuschel et al. showed conclusively that methylation data generated by Nanopore sequencing of tissue samples can be integrated with methylation array data and developed NanoDx, a machine-learning algorithm, which is able to distinguish different brain tumor entities. We show here that cfDNA methylation profiles generated from CSF can also be processed and analyzed by NanoDx.

The cohort described here is limited by the small sample sizes for some entities. This is due to the rarity of some entities and the use of CSF supernatants of samples from routine CSF diagnostics, which is not performed for all brain tumors. Still, our proof-of-concept study demonstrates that Nanopore sequencing is a highly valuable tool for CNS tumor diagnosis using liquid biopsies of CSF. We detected ctDNA in samples from benign as well as malignant brain tumors from different tumor entities and disease states. Only a small proportion of these samples had detectable tumor cells in the CSF, showing the additional value of using cfDNA as compared to microscopy of potential tumor cells. In summary, we show here that Nanopore sequencing of cfDNA from CSF for diagnosing and monitoring of brain tumors holds great potential to be integrated into routine diagnostics.

Data Availability

The data generated in this study are available upon reasonable request from the corresponding author.

Supplemental Material

Supplemental material is available at *Clinical Chemistry* online.

Nonstandard Abbreviations: CNS, central nervous system; cfDNA, cell-free DNA; CSF, cerebrospinal fluid; CNV, copy number variation; ctDNA, circulating tumor DNA.

Human Genes: C19MC, C19MC microRNA cluster, cluster of 46 genes; CTNNB1, beta catenin 1.

Author Contributions: The corresponding author takes full responsibility that all authors on this publication have met the following required criteria of eligibility for authorship: (a) significant contributions to the conception and design, acquisition of data, or analysis and interpretation of data; (b) drafting or revising the article for intellectual content; (c) final approval of the published article; and (d) agreement to be accountable for all aspects of the article thus ensuring that questions related to the accuracy or integrity of any part of the article are appropriately investigated and resolved. Nobody who qualifies for authorship has been omitted from the list.

Authors' Disclosures or Potential Conflicts of Interest: Upon manuscript submission, all authors completed the author disclosure form.

Research Funding: U. Schüller was generously supported by the Fördergemeinschaft Kinderkrebszentrum Hamburg and the Wilhelm-Sander Stiftung. C. Rohrandt, M. Synowitz, B. Brändl, and F.-J. Müller were supported by the German Federal Ministry for Research and Education (BMBF IntraEpiGliom, FKZ 13GW0347B, 13GW0347C, and 13GW0347D). S. Rutkowski, German Children's Cancer Foundation (funding of trial). B. Brändl and F.-J. Müller were partly supported by the Deutsche Forschungsgemeinschaft (German Research Foundation) under Germany's Excellence Strategy-EXC 22167-390884018 and by an intramural grant of the University Comprehensive Cancer Center Schleswig-Holstein (UCCSH Twinning 2022).

Disclosures: C. Rohrandt, B. Brändl, and F.-J. Müller, patent pending: PCT/EP2022/074773, "Method for the Diagnosis and/or Classification of a Diseases in a Subject." S. Rutkowski received consulting fees from Bayer (Advisory Board), Novartis (Advisory Board), BMS (Advisory Board), Roche (Advisory Board), Celgene (DMSC), German Children's Cancer Foundation (Assessment), MyChildsCancer (Consulting), and support for meeting attendance from the German Society for Pediatric Oncology and Hematology and German Children's Cancer Foundation. M. Sönksen received a scholarship from the German Academic Scholarship Foundation (Studienstiftung des deutschen Volkes). A.K. Wefers is a fellow of the Mildred Scheel Cancer Career Center Hamburg/Deutsche Krebshilfe. A.-K. Afflerbach received support from the interdisciplinary graduate school "Innovative Technologies in Cancer Diagnostics and Therapy" funded by the City of Hamburg.

Role of Sponsor: The funding organizations played no role in the design of study, choice of enrolled patients, review and interpretation of data, preparation of manuscript, or final approval of manuscript.

Acknowledgments: We express our gratitude to our patients and their families, who graciously shared biosamples enabling our work. We thank Nicole Borgardt, Helena Gladkov, Vanessa Thaden, Jacqueline Tischendorf, and Kerstin Sandner for excellent technical assistance. We are grateful to Ulrich Jetzek for helpful discussions and organizational support.

References

1. Louis DN, Perry A, Wesseling P, Brat DJ, Cree IA, Figarella-Branger D, et al. The 2021 WHO classification of tumors of the central nervous system: a summary. *Neuro Oncol* 2021;23:1231–51.
2. Capper D, Jones DTW, Sill M, Hovestadt V, Schrimpf D, Sturm D, et al. DNA methylation-based classification of central nervous system tumours. *Nature* 2018;555:469–74.
3. Alix-Panabières C, Pantel K. Liquid biopsy: from discovery to clinical application. *Cancer Discov* 2021;11:858–73.
4. Müller C, Holtschmidt J, Auer M, Heitzer E, Lamszus K, Schulte A, et al. Hematogenous dissemination of glioblastoma multiforme. *Sci Transl Med* 2014;6:247ra101.
5. Bettegowda C, Sausen M, Leary RJ, Kinde I, Wang Y, Agrawal N, et al. Detection of circulating tumor DNA in early- and late-stage human malignancies. *Sci Transl Med* 2014;6:224ra24.
6. Pentsova EI, Shah RH, Tang J, Boire A, You D, Briggs S, et al. Evaluating cancer of the central nervous system through next-generation sequencing of cerebrospinal fluid. *J Clin Oncol* 2016;34:2404–15.
7. Escudero L, Llort A, Arias A, Diaz-Navarro A, Martínez-Ricarte F, Rubio-Perez C, et al. Circulating tumour DNA from the cerebrospinal fluid allows the characterisation and monitoring of medulloblastoma. *Nat Commun* 2020;11:5376.
8. Liu APY, Smith KS, Kumar R, Paul L, Biannic L, Lin T, et al. Serial assessment of measurable residual disease in

- medulloblastoma liquid biopsies. *Cancer Cell* 2021;39:1519–1530.e4.
9. Martignano F, Munagala U, Crucitta S, Mingrino A, Semeraro R, Del Re M, et al. Nanopore sequencing from liquid biopsy: analysis of copy number variations from cell-free DNA of lung cancer patients. *Mol Cancer* 2021;20:32.
 10. Katsman E, Orlanski S, Martignano F, Fox-Fisher I, Shemer R, Dor Y, et al. Detecting cell-of-origin and cancer-specific methylation features of cell-free DNA from nanopore sequencing. *Genome Biol* 2022;23:158.
 11. De Coster W, D'Hert S, Schultz DT, Cruts M, Van Broeckhoven C. Nanopack: visualizing and processing long-read sequencing data. *Bioinformatics* 2018;34:2666–9.
 12. Li H. Minimap2: pairwise alignment for nucleotide sequences. *Bioinformatics* 2018;34:3094–100.
 13. Li H. New strategies to improve minimap2 alignment accuracy. *Bioinformatics* 2021;37:4572–4.
 14. Danecek P, Bonfield JK, Liddle J, Marshall J, Ohan V, Pollard MO, et al. Twelve years of SAMtools and BCFtools. *GigaScience* 2021;10:giab008.
 15. Boeva V, Popova T, Bleakley K, Chiche P, Cappo J, Schleiermacher G, et al. Control-FREEC: a tool for assessing copy number and allelic content using next-generation sequencing data. *Bioinformatics* 2012;28:423–5.
 16. Simpson JT, Workman RE, Zuzarte PC, David M, Dursi LJ, Timp W. Detecting DNA cytosine methylation using nanopore sequencing. *Nat Methods* 2017;14:407–10.
 17. Kuschel LP, Hench J, Frank S, Hench IB, Girard E, Blanluet M, et al. Robust methylation-based classification of brain tumours using nanopore sequencing. *Neuropathol Appl Neurobiol* 2023;49:e12856.
 18. Adalsteinsson VA, Ha G, Freeman SS, Choudhury AD, Stover DG, Parsons HA, et al. Scalable whole-exome sequencing of cell-free DNA reveals high concordance with metastatic tumors. *Nat Commun* 2017;8:1324.
 19. Baroni LV, Sundaresan L, Heled A, Coltin H, Pajtler KW, Lin T, et al. Ultra high-risk PFA ependymoma is characterized by loss of chromosome 6q. *Neuro Oncol* 2021;23:1360–70.
 20. Seoane J, De Mattos-Arruda L, Le Rhun E, Bardelli A, Weller M. Cerebrospinal fluid cell-free tumour DNA as a liquid biopsy for primary brain tumours and central nervous system metastases. *Annals Oncol* 2019;30:211–8.
 21. Miller AM, Shah RH, Pentsova EI, Pourmaleki M, Briggs S, Distefano N, et al. Tracking tumour evolution in glioma through liquid biopsies of cerebrospinal fluid. *Nature* 2019;565:654–8.
 22. Drexler R, Schüller U, Eckhardt A, Filipski K, Hartung TI, Harter PN, et al. DNA methylation subclasses predict the benefit from gross total tumor resection in IDH-wildtype glioblastoma patients. *Neuro Oncol* 2023;25:315–25.
 23. Thompson EM, Hielscher T, Bouffet E, Remke M, Luu B, Gururangan S, et al. Prognostic value of medulloblastoma extent of resection after accounting for molecular subgroup: a retrospective integrated clinical and molecular analysis. *Lancet Oncol* 2016;17:484–95.
 24. Ramaswamy V, Hielscher T, Mack SC, Lassaletta A, Lin T, Pajtler KW, et al. Therapeutic impact of cytoreductive surgery and irradiation of posterior Fossa ependymoma in the molecular era: a retrospective multicohort analysis. *J Clin Oncol* 2016;34:2468–77.
 25. Mouliere F, Mair R, Chandrananda D, Marassi F, Smith CG, Su J, et al. Detection of cell-free DNA fragmentation and copy number alterations in cerebrospinal fluid from glioma patients. *EMBO Mol Med* 2018;10:e9323.
 26. Maass KK, Schad PS, Finster AME, Puranachot P, Rosing F, Wedig T, et al. From sampling to sequencing: a liquid biopsy pre-analytic workflow to maximize multi-layer genomic information from a single tube. *Cancers (Basel)* 2021;13:3002.
 27. Zuccato JA, Patil V, Mansouri S, Voisin M, Chakravarthy A, Shen SY, et al. Cerebrospinal fluid methylome-based liquid biopsies for accurate malignant brain neoplasm classification. [Epub ahead of print] *Neuro Oncol* December 1, 2022 as doi: 10.1093/neuonc/noac264.
 28. Nassiri F, Chakravarthy A, Feng S, Shen SY, Nejad R, Zuccato JA, et al. Detection and discrimination of intracranial tumors using plasma cell-free DNA methylomes. *Nat Med* 2020;26:1044–7.
 29. Sahm F, Schrimpf D, Jones DTW, Meyer J, Kratz A, Reuss D, et al. Next-generation sequencing in routine brain tumor diagnostics enables an integrated diagnosis and identifies actionable targets. *Acta Neuropathol* 2016;131:903–10.
 30. Euskirchen P, Bielle F, Labreche K, Kloosterman WP, Rosenberg S, Daniau M, et al. Same-day genomic and epigenomic diagnosis of brain tumors using real-time nanopore sequencing. *Acta Neuropathol* 2017;134:691–703.